EFFECTS OF THERMAL AND ACID TREATMENTS ON SOME PHYSICO-CHEMICAL PROPERTIES OF LAMPANG DIATOMITE

Aphiruk Chaisena* **and Kunwadee Rangsriwatananon**

Recived: Apr 8, 2004; Revised: Aug 18, 2004; Accepted: Oct 6, 2004

Abstract

The physico-chemical properties of the natural diatomite, mined in the Lampang Province of Thailand, and the treated diatomite were studied. There included the composition analysis, phase analysis, morphology, thermal analysis, and particle size analysis. The results showed that the natural diatomite was composed of mainly amorphous silica (Opal A) and a small amount of quartz. The calcination did not change the Si/Al molar ratio but the particle size distribution decreased when the temperature was increased. The hot acid treatment affected both the chemical composition and the structure. The hot H_2SO_4 treated diatomite followed by calcination in the range of 900 - 1,100°C did not result in crystallization of cristobalite. The diatomite treated with hot 6 M H_2SO_4 then calcined at 1,100°C could be utilized as catalyst supports and adsorbent because it contained high amorphous silica and lower impurity.

Keywords: Diatomite, amorphous silica, calcination, acid treatment

Introduction

Diatomite is a siliceous, sedimentary rock consisting principally of fossilized skeletal remains of diatoms, unicellular aquatic plants related to algae. The skeletons are essentially amorphous hydrated or opaline silica but occasionally are partly composed of alumina. Sometimes the deposits consist of diatom shells only, but usually diatomite contains other sediments such as clay and fine sand. Since diatoms are composed of an amorphous form of silica containing a small amount of microcrystalline material, diatomite is chemically stable and inert. Because of the open structure of diatom skeletons, diatomite is a lightweight rock and yet quite hard. Diatomite (also known as diatomaceous earth, *Kieselguhr*, tripolite, etc.) is easily available in large quantities at an extremely low cost (Biswajit *et al.*, 1994). The type of silica present in diatomite is a hydrous form of opaline silica, which contains between 3 - 8% structural water. The important properties of diatomite are related to physical structures and an aggregate of fine particles perforated by a regular pattern of very small holes. The honeycomb silica structure gives diatomite useful characteristics such as unique particulate structure, chemical stability, low bulk density, high absorptive capacity,

School of Chemistry, Institute of Science, Suranaree University of Technology, 111 University Avenue, Nakhon Ratchasima 30000, Thailand, Tel.: 0-1593-7184, E-mail: a_chaisena@hotmail.com

* *Corresponding author*

high surface area, and low abrasion. These characteristics enable the material to be commercially applicable as a filter aid, absorbent, anti-caking agent, thermal insulator, filler and extender, catalyst carrier, chromatographic support and additive for numerous other purposes. In Thailand, diatomite is mainly found in the Lampang Province but its physico-chemical properties (particle, composition, phase, morphology) are not good enough for wide use unless it is modified (Inglethorpe *et al.*, 1997).

The aim of this study was to develop treated Lampang diatomite for a wider range of application. The characteristic features, mineralogical structure and the effects of the processing including thermal and acid treatments were investigated.

Materials and Methods

Materials

The used diatomite sample was collected from Ban Keuw in Mae Tha District of the Lampang Province, northern Thailand. It came from the deposit of the Lampang Basin. The deposition started with Miocene sandstone, lignite, mudstone, shale and oil shale of the Mae Sot Formation, which gave way to Pliocene diatomite, diatomaceous clay and silty clay of the Ko Kha Formation (Owen and Utha-aroon, 1999). The collected diatomite was crushed to aggregate-size pieces in roller mills with air-drying, and was ground to less than 63 μm by hand before further treatment.

Methods

The natural diatomite was submitted to calcination at 900, 1,000, and 1,100°C to give the calcined diatomite. Calcination was carried out under an air atmosphere in a programmable furnace, with a heating rate from room temperature to the calcination temperature of 16°C.min^{-1}, and the samples were left in the furnace for 5 h at the calcination temperature. These solids were kept for characterization and one part of them was submitted to acid treatment. The acid treatments were carried out with 6 M H_2SO_4, 6 M HCl, and 6 M HNO_3 solutions, at room temperature for 24, 72, 120, 168 h and at about 100°C for 1, 6, 12, 24 h with reflux conditions. The natural diatomite of 10 g was mixed with 50 mL of the acid solutions and stirred during the times indicated above. Consequently, the suspensions were centrifuged and the solids were washed with deionized water until the washed water to pH = 7 and dried at 100°C for 12 h. The total dissolution percentages of material were calculated from difference in weight between the starting and undissolved materials (filter cake). Thermal and acid treatment, samples were obtained by using the natural diatomite was submitted to calcination at 900, 1,000, and 1,100°C for 5 h and followed by reflux with 6 M H_2SO_4 at about 100°C for 124 h. For the acid and thermal treatment, samples were prepared by reflux with 6 M H_2SO_4 at about 100°C for 24 h and then calcined at 900, 1,000, and 1,100°C for 5 h.

Samples for scanning electron microscopy (SEM) (model JSM 6400) were prepared by dispersing. They were put on to a conductive carbon tape and coated with gold to prevent charging in order to observe the fine detail of the diatomite skeletons. Their particle size distributions were measured by laser light-scattering-based particle sizer (Malvern Mastersizer S Ver 2.15) with wet method using water as a medium to disperse the samples. The solution was ultrasonicated in order to break down the flocculates before the run was made. Elemental analyses of the samples were carried out by wavelength dispersive X-ray fluorescence (WDXRF) model Philips PW 2404, MagiX Pro. Examinations were carried out on the basis of calibration curves which were made with the use of certified reference materials; kaolin (MBH reference materials), 600 (bauxite), 679 (brick clay), 98b (plastic clay) and 2,709 (soil). Fused tetraborate matrix X-ray fluorescence method was used to determine the total element contents of the natural diatomite and the treated diatomite. The tube high voltage was 40 kV with the tube current of 30 mA. X-ray powder diffraction patterns were obtained by using Bruker D5005 powder diffractometer, operated at 35 kV and 35 mA, and employing Cu Kα filtered radiation.

The sample was placed into a cylindrical hollow Al holder. The X-ray scans were run at 0.3 degree/0.02 second. The thermogravimetric (DTA/TGA/TGA) analyses were carried out by Analyzer Simultaneous TGA-DTA Instrument model SDT-2960 at a heating rate of 16°C.min^{-1} under a flow of oxygen of 20 L.min^{-1} with Al_2O_3 as a reference for the measurement. The thermal analyses curves were recorded simultaneously along with temperature increment. FT-IR (Perkin-Elmer spectrum GX) spectra were recorded in the region of 4,000-370 cm^{-1} with the KBr pellet technique. About 1 mg of the sample and 300 mg of KBr were used in the preparation of the pellets.

Results and Discussion

The SEM micrograph of the natural diatomite given in Figure 1 is typical, showing dominant *A. granulata* species. It has an average particle size of 9.88 μm. It was found to be essentially amorphous (single band centered at approximately 22° 2θ (4.1 Å d-spacing)) but also contained a small amount of quartz, kaolinite, montmorillonite and illite which was indicated by the XRD pattern (Figure 2). The percentages of chemical weight of the natural diatomite were as follows: SiO_2, 71.90; Al_2O_3, 14.60; Fe_2O_3, 5.78; K_2O, 1.95; CaO, 0.17; MgO, 0.69; MnO, 0.01; TiO_2, 0.51 and the Si/Al ratio was 4.35. FT-IR spectrum of the natural diatomite was shown in Figure 3 and the interpretation of this spectrum has been guided by the data published in literatures (Van der

Figure 1. SEM micrograph showing the diatom skeletons.

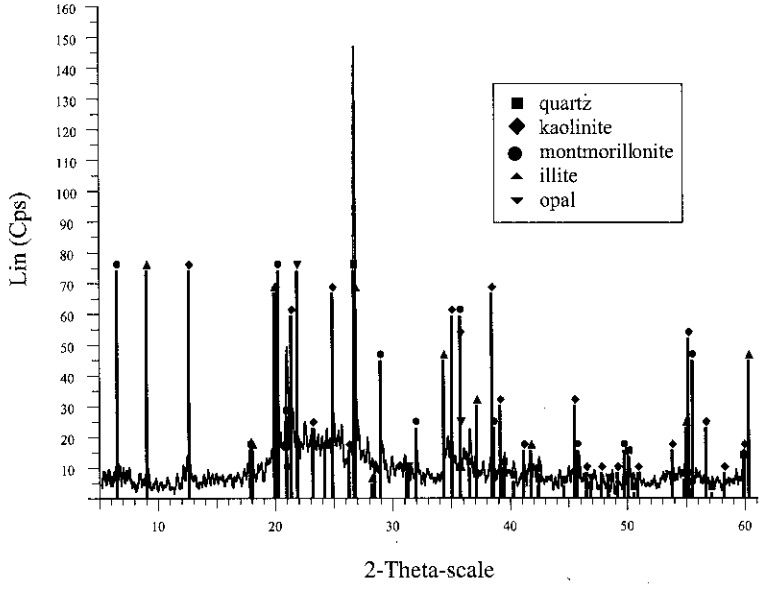

Figure 2. XRD pattern of the natural diatomite compared with the standard pattern from JCPDS database.

Marel and Beutelspacher, 1976; Hassan *et al.*, 1999; Weng *et al.*, 1999; Al-Degs *et al.*, 2001; Yuan *et al.*, 2001; Aicha *et al.*, 2003). The identification of IR absorption bands related to vibrations is shown in Table 1. The thermogravimetric analyses (DTA/TGA/TGD) of the natural diatomite are shown in Figure 4. The DTA curve showed three endothermic effects at 76.7, 496.2 and 1,086°C accompanied the weight loss of TGA curve. The endothermic peak centered at 76.7°C and a shoulder around 165°C were assigned to the loss of water absorbed on the diatomite. The small peak at 496.2°C might be due to the liberation of water caused by dehydroxylation of some associated silanol groups on the external surface of the diatomite. In the high temperature region, the large endothermic peak with a centre at 1,086°C has been assigned to a formation of siloxane bridges resulting from dehydroxylation of isolated silanol groups on the internal surface of the diatomite. As the results of the evaporation, (1) new voids appear, and (2) defects occur in the crystalline structures (Goren *et al.*, 2002). During this process the diatomite loses the hydroxyl units from its structure and an amorphous product is formed (Biswajit *et al.*, 1994).

Thermal Treatment

The effect of temperature on a particle size distribution showed that the average size of

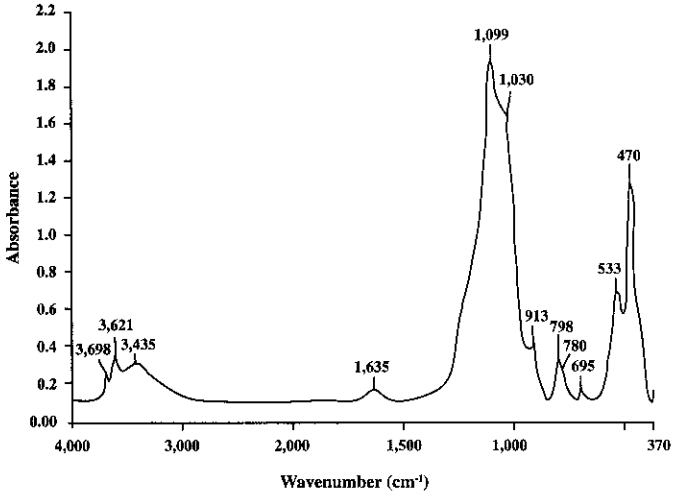

Figure 3. FT-IR spectra of the natural diatomite.

Table 1. Identification of IR absorption bands to specific vibrations.

Wavenumber (cm^{-1})	Vibrations
3,698 and 3,621	O-H stretching of kaolinite
3,435	O-H stretching of water
1,635	H_2O bending
1,099 and 1,030	Si-O-Si stretching
913	Si-OH stretching, Al-Al-OH bending (kaolinite)
798 and 780	Intertetrahedral Si-O-Si bending
695 and 470	O-Si-O bending
533	Si-O-Al bending

particle decreased with increasing temperature. It was found that the average particle size of the calcined diatomite at 900, 1,000, and 1,100°C is 18.15, 17.16, and 16.82 μm, respectively. The color of the natural diatomite becomes pink or yellowish to dark brown due to iron contents converted into Fe_2O_3. The results of the chemical analyses of the three calcined diatomite samples (900, 1,000 and 1,100°C), given in Table 2, indicated that the main chemical compositions contain oxides of Si and Al together with other mineral impurities i.e. Fe, K, Ca, Mg, etc. The Si/Al ratio and the other mineral impurities of natural diatomite and calcined diatomite slightly differ. The percentage of chemical composition of the natural diatomite is not equal to 100 because of the content of water and organic substances which can be removed by calcination and acid treatment (Bibliothek, 1998). The X-ray diffraction analyses of these calcined diatomite samples are shown in Figure 5. The XRD patterns of the calcined diatomite at 900°C show an additional peak at 19.8° 2θ, beside the peak of quartz at 26.65° 2θ and 20.86° 2θ. The new peak at 19.8° 2θ was assigned to be a tectosilicates structure (Mollah *et al.*, 1999). A new peak appeared at 21.8° 2θ in the calcined diatomite at 1,100°C, was corresponded to crystals of cristobalite (Calacal and Whittemore, 1987). FT-IR spectra of the calcined diatomite samples are shown in Figure 6. These spectra confirmed that the calcination at any conditions in this experiment

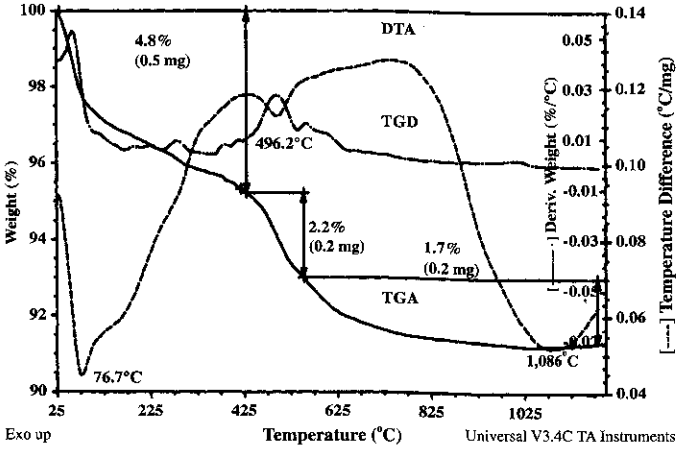

Figure 4. The thermogravimetric (DTA/TGA/TGD) curves for the natural diatomite material.

Table 2. The chemical compositions and Si/Al ratios of calcined diatomite compared with natural diatomite determined by XRF.

Chemical content (% weight)	Natural diatomite	Calcination at 900°C	Calcination at 1,000°C	Calcination at 1,100°C
SiO_2	71.90	76.34	76.24	76.73
Al_2O_3	14.60	15.43	15.26	15.48
Fe_2O_3	5.78	6.08	6.08	6.18
K_2O	1.95	1.96	1.91	1.92
CaO	0.17	0.17	0.23	0.17
MgO	0.69	0.75	0.79	0.75
MnO	0.01	0.01	0.01	0.01
TiO_2	0.51	0.53	0.52	0.52
Si/Al ratio	4.35	4.37	4.40	4.38

produced dehydroxylation in the diatomite samples i.e. elimination of the OH stretching from Si-OH and Al-Al-OH bond at 913 cm^{-1} (Belver *et al.*, 2002; Shawabkeh and Tutunji, 2003). In the region of OH stretching vibration of water, it showed a band at 3,436 cm^{-1}, which is typical of water forming hydrogen bond on the diatomite and remained in all samples after the calcination. A weak additional band, assigned to the H-O-H bending vibration mode of H_2O adsorbed molecules, can be seen at 1,635 - 1,623 cm^{-1}. The OH stretching band of kaolinite at 3,698 and 3,621 cm^{-1} were eliminated in all samples after the calcination. The absorption band at 533 cm^{-1}, which is related to Al at octahedral sheet (Si-O-Al bending) of kaolin (Belver *et al.*, 2002), was not observable even after being calcined at 900, 1,000 and 1,100°C. This is because the octahedral sheet changed into tetrahedral sheet of metakaolin (Belver *et al.*, 2002). For the calcination at 900°C, it showed mullite structure and a part of

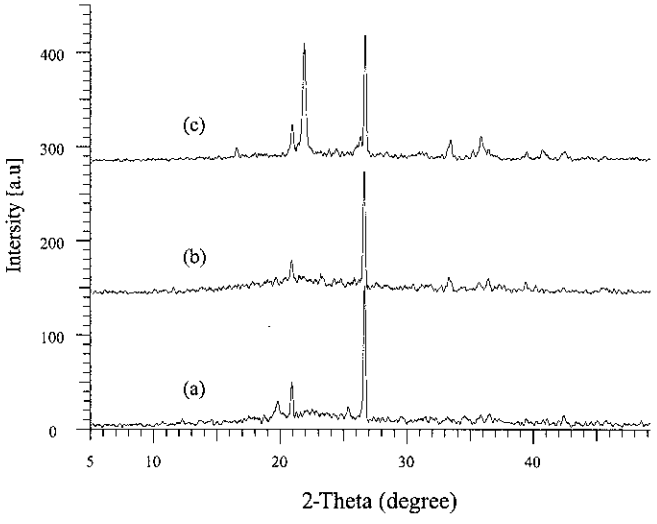

Figure 5. XRD patterns of the calcined diatomite (a) 900°C (b) 1,000°C and (C) 1,100°C.

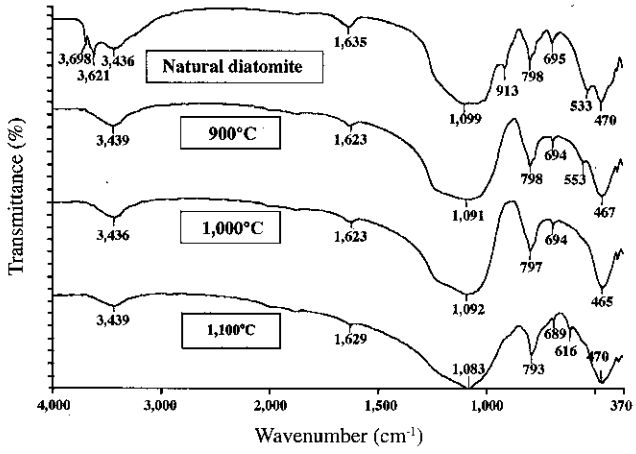

Figure 6. IR spectra at 900, 1,000, and 1,100°C compared with the natural diatomite sample.

metakaolin with a band at 553 cm^{-1} (Ojima, 2003). The appearance of a new band at 616 cm^{-1} when calcination at 1,100°C showed the typical of cristobalite.

The SEM micrographs of the calcined diatomite at 900 and 1,000°C (Figure 7) gave details of diatomite structure, which is still the original geometry. After calcined at 1,100°C, the material still showed signs of its original diatomite structure, but the concave and convex surfaces were almost gone, and smoother surfaces were formed instead.

Acid Treatment

The total dissolution percentages of the activated samples by acids are shown in Figure 8. Their chemical compositions after the acid activation determined by XRF are tabulated in Table 3. The percentage of the weight of dissolved substances changes much more rapidly with the hot acid than the cold acid condition. The maximum extent of dissolution was obtained with the hot acid solutions and the highest silica (SiO_2) content was obtained from the natural diatomite activated with hot 6 M H_2SO_4 for 24 h. It is well known that many acids dissolve certain substances in diatomite and alter their chemical compositions (Hassan *et al.*, 1999; Goren *et al.*, 2002). The obtained dissolutions treated with 6 M hot acid for 24 h contained great amounts of the soluble oxides. The high solubility may result from the appearance of the soluble oxides in contact with the solvent acid due to the destruction of the physical structure of diatom and other particles. Again, significant amounts of amorphous silica may be dissolved together with alumina when the activation time is increased (Goren *et al.*, 2002). In the

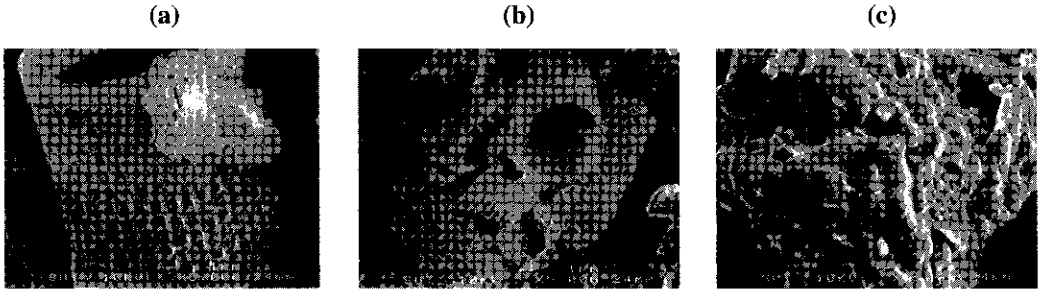

Figure 7. SEM micrographs of the calcined diatomite obtained after calcination at (a) 900°C (b) 1,000°C and (c) 1,100°C.

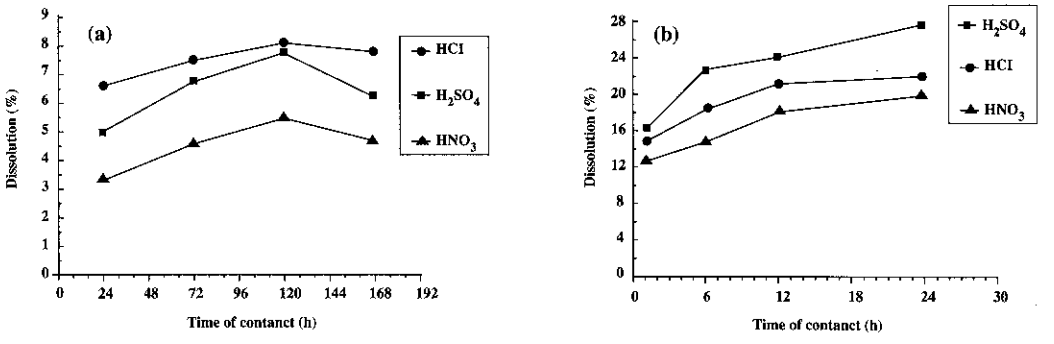

Figure 8. The total dissolution percentages of the material in cold acid (a) and hot acid (b) conditions.

conditions of cold acid treatments after 120 hs, the percentage of total dissolution trends to decrease. This may be due to the limited solubility of impurities, and the formation of some insoluble metallic oxides complexes of SO_4^{2-}, Cl^-, and NO_3^-. From Figure 9 showing the XRD patterns of the diatomite treated with hot acid, they revealed amorphous silica and the presence of quartz. This suggests that the acid activation does not change the diatomite structure and quartz. FT-IR spectra of hot acid treatment samples were shown in Figure 10. The IR band intensities of Si-OH or Al-Al-OH at 913 cm^{-1} and Si-O-Al, which is related to Al octahedral sheet found at 533 cm^{-1}, decreased more rapidly when the diatomite was activated with hot HCl 6 M than with hot HNO_3 6 M. These bands were eliminated with hot H_2SO_4 6 M for 24 h. This trend can be seen in the region of OH stretching vibration of kaolinite (3,698 and 3,621 cm^{-1}) as well. The results indicate that clay minerals can be removed more easily with hot H_2SO_4 than with others. The SEM micrographs of the acid activated diatomite in Figure 11 showed that the original geometry of the pores was preserved but there was a collapse

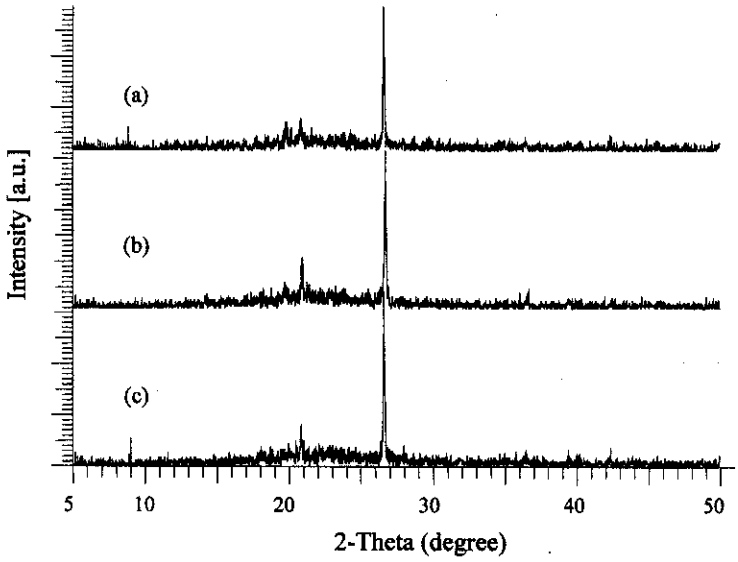

Figure 9. XRD patterns of the natural diatomite treated with (a) hot 6 M HNO_3 (b) hot 6 M HCl and (c) hot 6 M H_2SO_4 for 24 h.

Table 3. The chemical compositions at the maximum dissolution conditions and Si/Al ratios of acid activated diatomite compared with natural diatomite determined by XRF.

Material	Chemical content (% weight)								Si/Al ratio
	SiO_2	Al_2O_3	Fe_2O_3	K_2O	CaO	MgO	MnO	TiO_2	
Natural diatomite	71.90	14.60	5.78	1.95	0.17	0.69	0.01	0.51	4.35
Cold, H_2SO_4 6 M, 120 h	75.83	14.86	4.01	1.97	0.00	0.51	0.00	0.52	4.50
Cold, HCl 6 M, 120 h	75.57	14.89	3.19	1.97	0.00	0.50	0.00	0.52	4.48
Cold, HNO_3 6 M, 120 h	73.27	14.69	5.44	1.87	0.00	0.51	0.00	0.51	4.40
Hot, H_2SO_4 6 M, 24 h	93.56	3.63	0.53	0.80	0.00	0.16	0.00	0.46	22.77
Hot, HCl 6 M, 24 h	91.14	5.34	0.60	1.12	0.00	0.20	0.00	0.53	15.10
Hot, HNO_3 6 M, 24 h	86.60	8.54	0.85	1.63	0.00	0.32	0.00	0.57	8.96

of the skeletal structure.

Thermal and Acid Treatments

X-ray diffraction analyses of the natural diatomite treated with both thermal and hot acid are shown in Figure 12 and Table 4. It showed that only amorphous silica and some of quartz appeared when the diatomite samples were treated under almost all conditions studied, except for two conditions i.e. the treatment with calcination at 1,100°C and the treatment with calcination at 1,100°C then followed by hot 6 M H_2SO_4. In the latter cases, the peak of critobalite also occurred. This suggests that the two samples contained some impurities, which caused crystallization. The diatomite obtained from treatment firstly with hot 6 M H_2SO_4 then calcination at 1,100°C could be utilized as catalyst support and adsorbent because of its contents of higher amorphous silica and lower impurity (Emilio *et al.*, 1993).

Conclusions

The type of silica presented in the natural diatomite is a poorly-ordered opal A type and a small amount of quartz. When the natural

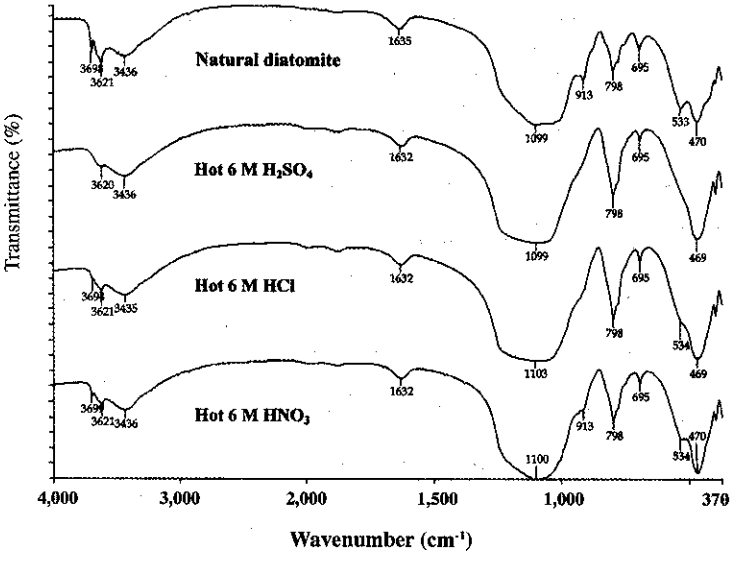

Figure 10. IR transmission spectra of the natural diatomite after treated with hot acid.

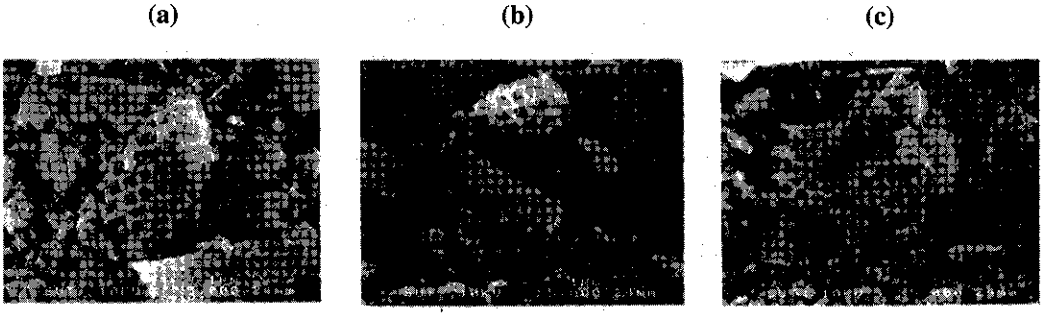

Figure 11. SEM showing structure in the natural diatomite treated with hot reflux (a) 6 M H_2SO_4 (b) 6 M HCl and (c) 6 M HNO_3 for 24 h.

diatomite was calcined with different temperatures in the range of 900 - 1,100°C, the Si/Al ratio and other mineral impurities slightly differ. After the calcination, the colour of the products is pink or yellowish to dark brown because iron impurities changed into Fe_2O_3. The particle size distribution decreases when temperature is increased. Some amorphous phases of the natural diatomite can be transformed into crystalline structure of cristobalite at 1,100°C. The morphology of the calcined diatomite at 1,100°C still showed original diatomite structure, but with smoother surface than the treated diatomite at 900 and 1,000°C. It was found that the hot acid affected both the composition and the structure, while the cold acid affected only the composition. The total dissolutions of the natural diatomite were increased with increasing temperatures and time. Cristobalite did not appear in the samples treated

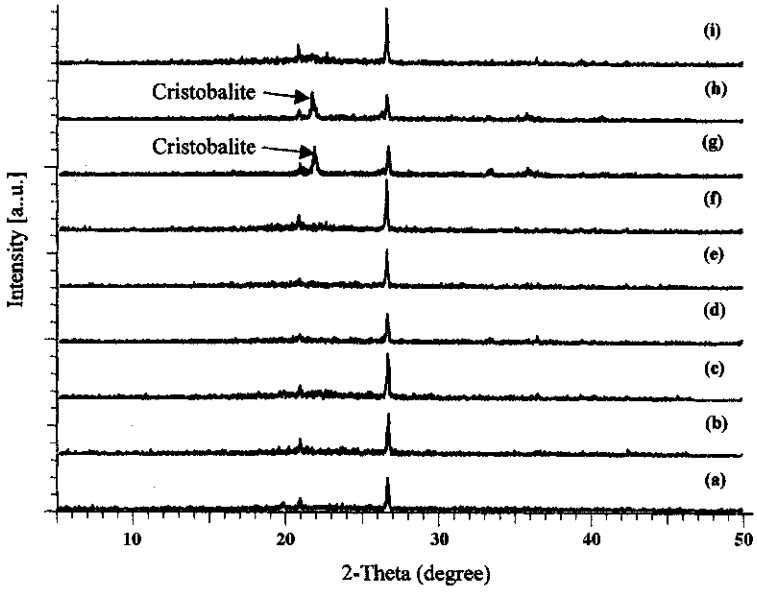

Figure 12. XRD patterns of (a) diatomite calcined at 900°C (b) diatomite calcined firstly at 900°C then treated with hot 6 M H_2SO_4 (c) diatomite treated firstly with hot 6 M H_2SO_4 then calcined at 900°C (d) diatomite calcined at 1,000°C (e) diatomite calcined firstly at 1,000°C then treated with hot 6 M H_2SO_4 (f) diatomite treated firstly with hot 6 M H_2SO_4 then calcined at 1,000°C (g) diatomite calcined at 1,100°C (h) diatomite calcined firstly at 1,100°C then treated with hot 6 M H_2SO_4 and (i) diatomite treated firstly with hot 6 M H_2SO_4 then calcined at 1,100°C.

Table 4. X-ray diffraction analyses of thermal and acid treatment of natural diatomite samples.

Temperature (°C)	Natural diatomite	Calcined-treated with H_2SO_4	Treated with H_2SO_4-calcined
900	amorphous	amorphous	amorphous
1,000	amorphous	amorphous	amorphous
1,100	cristobalite	cristobalite	amorphous

with hot H_2SO_4, while only the treatment of diatomite at 1,100°C caused crystallization of cristobalite.

Acknowledgements

The authors wish to acknowledge the financial support from the Office of Rajabhat Institute Council (ORIC) and the Suranaree University of Technology.

References

Aicha, G-B., Thibaud, C., Jocelyne, M., and Jacques, L. (2003). Spectroscopic characterization of biogenic silica. J. Non-Cryst. Solids., 316:331-337.

Al-Degs, Y., Khraisheh, M.A.M., and Tutunji, M.F. (2001). Sorption of lead ions on diatomite and manganese oxides modified diatomite. Wat., Res. 35:3,724-3,728.

Belver, C., Munoz, M.A.B., and Vicente, M.A. (2002). Chemical activation of a kaolinite under acid and alkaline condition. Chem. Mater., 14:2,033-2,043.

Bibliothek, D.D. (1998). Industrial inorganic chemicals and products. 5:4,059.

Biswajit, G., Dinesh, C., and Subhash, B. (1994). Synthesis of zeolite A from calcined diatomaceous clay: optimization studies. Ind. Eng. Chem. Res., 33:2, 107-2,110.

Calacal, E.L., and Whittemore, O.J. (1987). The sintering of diatomite. Am. Ceram. Soc. Bull., 66(5):790-793.

Emilio, G., Isabel, G., Eduardo, M., and Adolfo, M. (1993). Properties and applications of diatomitic materials from SW Spain. Appl. Clay. Sci., 8:1-18.

Goren, R., Baykara, F., and Marsoglu, M. (2002). A study on the purification of diatomite in hydrochloric acid. Scand. J. Metall., 31:115-119.

Hassan, M.S., Ibrahim, I.A., and Ismael, I.S. (1999). Diatomaceous Deposits of Fayium Egypt; characterization and evaluation for industrial application. Chin. J. Geochem., 18:233-240.

Inglethorpe, S.D.J., Utha-aroon, C., and Chanyavanich, C. (1997). An inventory of diatomite deposits of the Lampang Basin, northern Thailand. Proceedings of the International Conference on Stratigraphy and Tectonic Evolution of Southeast Asia and South Pacific; August 19-24, 1997; Bangkok, Thailand, 17 p.

Mollah, M.Y.A., Promreuk, S., Schennach, R., Cocke, D.L., and Guler, R. (1997). Cristobalite formation from thermal treatment of Texas linite fly ash. Fuel., 78:1,277-1,282.

Ojima, J. (2003). Determining of crystalline silica in respirable dust samples by infrared spectrophotometry in the presence of interferences. J. Occup Health., 45:94-103.

Owen, R.B., and Utha-aroon, C. (1999). Diatomaceous sedimentation in the tertiary Lampang Basin, Northern Thailand. J. Paleolim., 22:81-95.

Shawabkeh, R.A., and Tutunji, M.F. (2003). Experimental study and modeling of basic dye sorption by diatomaceous clay. Appl. Clay. Sci., 24:111-120.

Van der Marel, H.W., and Beutelspacher, H. (1976). Atlas of Infrared Spectroscopy of Clay Minerals and Their Admixtures. Elsevier, New York, p. 275-279.

Weng, H., Shen, Z., Yuan, M., Guo, D., and Chen, J. (1999). Stability of diatomaceous silica and its geochemical implication. Chin. Sci. Bull., 44:2,205-2,208.

Yuan, P., Wu, D., Chen, Z., Diao, G., and Peng, J. (2001). ^1H MAS NMR spectra of hydroxyl species on diatomite surface. Chin. Sci. Bull., 46:1,118-1,121.